Asymmetric Wave Reflection in Kinematic and Dynamic Approaches to Description of Parametric X-Radiation of a Relativistic Electron in the Crystal

S. V. Blazhevich and A. V. Noskov

Belgorod State University, Belgorod, Russia

Received July 12, 2010

Abstract—Parametric X-radiation (PXR) of a relativistic electron travelling through a monocrystalline plate is examined in the Laue scattering geometry under the assumption of asymmetric and symmetric reflections of the particle field with respect to a target surface. The formulas of the kinematic and dynamic approaches to PXR characterization are analyzed and compared. The results of the experiment on relativistic electron PXR implemented at the Mainz microtron are interpreted using an expression derived for its angular distribution. It has been revealed for the first time that the dynamic effect of anomalous photoabsorption (the Bormann effect) of PXR has taken place in this experiment.

INTRODUCTION

When a charged particle travels through a monocrystal, its Coulomb field diffracts on the parallel atomic planes of a crystal, giving rise to parametric X-radiation (PXR) [1–3]. Today, there are kinematic [4, 5] and dynamic [2, 3, 6] approaches to PXR characterization. It should be noted that the kinematic approach only describes the interactions of each atom with a primary (refracted) wave in a crystal and, in contrast to the dynamic approach, ignores its interaction with the total wave field produced by scattering from all the other atoms of a crystal; i.e., the multiwave scattering effect (in particular, interaction between elementary waves and a refracted one) is not taken into consideration.

In the last few years, the dynamic theory has gained significant ground in describing coherent radiation of relativistic electrons in crystals [7–11]. A striking example confirming the validity and advisability of the dynamic approach to PXR is the experimental observation of PXR reflection along the relativistic electron velocity [12], which is not predicted by means of the kinematic theory.

It is well known that the reflection asymmetry of a field with respect to the surface of a crystalline plate markedly affects the spectral-angular density of radiation. According to the kinematic theory, only the ratio between the charged particle path in the crystalline plate and the emitted photon path is dependent on asymmetry. The dynamic theory of relativistic electron PXR also predicts the substantial influence of asymmetric reflections on radiation process as such, leading to a change in the PXR spectrum. Thus, a topical problem solved in this study is to determine the limits of applicability of the kinematic approach to relativistic electron PXR in crystals.

In subsequent sections, the formulas for PXR derived on the basis of kinematic and dynamic theories are analyzed and compared under conditions corresponding to thin and thick crystals with the aim of finding the criteria restricting an appropriate application of the kinematic formula.

SPECTRAL-ANGULAR DISTRIBUTION OF PARAMETRIC X-RADIATION IN THE DYNAMIC THEORY

The expressions describing the spectral-angular density of PXR from a thick absorbing crystal has been derived in [13] via the dynamic diffraction theory [14]:

$$\omega\frac{d^2N_{\mathrm{PXR}}^{(s)}}{d\omega d\Omega}=\frac{e^2}{4\pi^2}\frac{P^{(s)^2}\theta^2}{\left(\theta^2+\gamma^{-2}-\chi_0'\right)^2}R_{\mathrm{PXR}}^{(s)},\tag{1a}$$

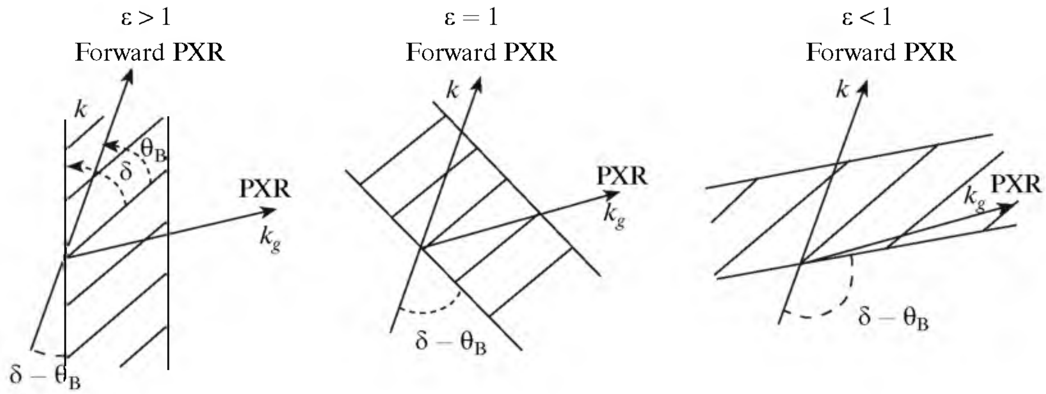

Fig. 1. Asymmetric radiation reflections from a crystalline plate at ε > 1 and ε < 1. The parameter (ε = 1 corresponds to symmetric reflection).

$$R_{\mathrm{PXR}}^{(s)} = \left(1 - \frac{\xi^{(s)}}{\sqrt{\xi^{(s)^2} + \varepsilon}}\right)^2 \frac{1 + \exp\left(-2b^{(s)}\rho^{(s)}\Delta^{(1)}\right) - 2\exp\left(-b^{(s)}\rho^{(s)}\Delta^{(1)}\right)\cos\left(b^{(s)}\left(\sigma^{(s)} + \frac{\xi^{(s)} - \sqrt{\xi^{(s)^2} + \varepsilon}}{\varepsilon}\right)\right)}{\left(\sigma^{(s)} + \frac{\xi^{(s)} - \sqrt{\xi^{(s)^2} + \varepsilon}}{\varepsilon}\right)^2 + \rho^{(s)^2}\Delta^{(1)^2}}. \quad (1b)$$

Here, notation conventions are analogous to those used in [13]:

$$\xi^{(s)}(\omega) = \eta^{(s)}(\omega) + \frac{1-\varepsilon}{2\nu^{(s)}},$$

$$\eta^{(s)}(\omega) = \frac{2\sin^2\theta_B}{V^2\left|\chi_g'\right|C^{(s)}}\left(1 - \frac{\omega(1 - \theta\cos\varphi\cot\theta_B)}{\omega_B}\right),$$

$$b^{(s)} = \frac{\omega\left|\chi_g'\right|C^{(s)}}{2}\frac{L}{\cos\psi_0}, \quad \rho^{(s)} = \frac{\chi_g''}{\left|\chi_g'\right|C^{(s)}}, \quad (2)$$

$$\Delta^{(s)} = \frac{\varepsilon+1}{2\varepsilon} - \frac{1-\varepsilon}{2\varepsilon}\frac{\xi^{(s)}}{\sqrt{\xi^{(s)^2} + \varepsilon}} - \frac{\kappa^{(s)}}{\sqrt{\xi^{(s)^2} + \varepsilon}},$$

$$\sigma^{(s)} = \frac{1}{\left|\chi_g'\right|C^{(s)}}\left(\theta^2 + \gamma^{-2} - \chi_0'\right), \quad \varepsilon = \frac{\cos\psi_g}{\cos\psi_0},$$

$$\nu^{(s)} = \frac{\chi_g' C^{(s)}}{\chi_0'}, \quad \kappa^{(s)} = \frac{\chi_g'' C^{(s)}}{\chi_0''}.$$

Since the inequality $2\sin^2\theta_B/V^2\left|\chi_g'\right|C^{(s)} \gg 1$ is valid in the X-ray frequency range, quantity $\eta^{(s)}(\omega)$ is the fast function of frequency ω. Hence, it is convenient to take $\eta^{(s)}(\omega)$ as a spectral variable in subsequent analysis of the PXR spectrum. Expression (1b) involves important parameter ε that determines the degree of asymmetry of field reflections in the crystal with respect to the plate surface. The wave vectors of incident and diffracted photons are directed at equal or unequal angles to the plate surface when a reflection process is, respectively, symmetric or asymmetric (Fig. 1). In the former case, $\varepsilon = 1$ and $\delta = \pi/2$. In the latter case, $\varepsilon \neq 1$ and $\delta \neq \pi/2$.

Let us write the asymmetry parameter as

$$\varepsilon = \frac{\sin(\delta + \theta_B)}{\sin(\delta - \theta_B)}, \quad (3)$$

where θ_B is the angle between the electron velocity and a set of crystallographic planes.

Note that the angle $\delta - \theta_B$ of electron incidence on the plate surface increases with decreasing parameter ε and vice versa (Fig. 1). As is known, asymmetry parameter (3) is the ratio between the electron path length in the plate $\left(L_{e^-} = \frac{L}{\sin(\delta - \theta_B)}\right)$ and the maximum photon path length in the crystal $\left(L_f = \frac{L}{\sin(\delta + \theta_B)}\right)$ after its formation near the input surface of a target.

Parameter $\nu^{(s)}$ characterizes the degree of wave reflection from a set of parallel atomic planes in the crystal, which is determined by the constructive ($\nu^{(s)} \approx 1$) or destructive ($\nu^{(s)} \approx 0$) interference of waves reflected from atoms of different atomic planes. Absorption parameter $\rho^{(s)}$ can be represented as the ratio of the X-ray wave extinction and absorption lengths in the crystal: $L_{\text{ext}}^{(s)}=\dfrac{1}{\omega\left|\chi_g'\right|C^{(s)}}$ and $L_{\text{abs}}=\dfrac{1}{\omega\chi_0''}$, respectively. It should be emphasized that the primary wave energy is completely transferred to a secondary wave propagating in the Bragg direction at the depth equal to the extinction length.

The solution to the equation

$$\sigma^{(s)}+\frac{\xi^{(s)}-\sqrt{\xi^{(s)^2}+\varepsilon}}{\varepsilon}=0 \tag{4}$$

determines the central frequency ω_*, of the spectrum of PXR photons emitted at a fixed observation angle.

Below, dynamic formula (1b) is compared with the well-known kinematic formula [4, 5]. In addition, we find criteria restricting the appropriate employment of the kinematic formula for PXR.

COMPARATIVE ANALYSIS OF KINETIC AND DYNAMIC FORMULAS: A THIN CRYSTAL

In the case of a thin target $\left(b^{(s)}\rho^{(s)}\ll 1\right)$, absorption coefficient $\rho^{(s)}$ can be ignored. Hence, expression (1b) describing the PXR spectrum takes the form

$$R_{\text{PXR}}^{(s)}=4\left(1-\frac{\xi^{(s)}}{\sqrt{\xi^{(s)^2}+\varepsilon}}\right)^2 \times\frac{\sin^2\left(\dfrac{b^{(s)}}{2}\left(\sigma^{(s)}+\dfrac{\xi^{(s)}-\sqrt{\xi^{(s)^2}+\varepsilon}}{\varepsilon}\right)\right)}{\left(\sigma^{(s)}+\dfrac{\xi^{(s)}-\sqrt{\xi^{(s)^2}+\varepsilon}}{\varepsilon}\right)^2}. \tag{5}$$

To observe pronounced dynamic effects, let us consider a crystalline plate such that the electron path length $L/\sin(\delta-\theta_B)$ within its thickness is many times greater than the X-ray wave extinction length $L_{\text{ext}}^{(s)}=\dfrac{1}{\omega\left|\chi_g'C^{(s)}\right|}$ in the crystal; i.e., $b^{(s)}\gg 1$. Integrating expression (1a) over frequency function $\eta^{(s)}(\omega)$, we obtain the formula for the PXR angular density:

$$\frac{dN_{\text{PXR}}^{(s)}}{d\Omega}=\frac{e^2\left|\chi_g'\right|C^{(s)}}{8\pi^2\sin^2\theta_B}\frac{P^{(s)^2}\theta^2}{(\theta^2+\gamma^{-2}-\chi_0')^2} \times\int_{-\infty}^{+\infty}R_{\text{PXR}}^{(s)}d\eta^{(s)}(\omega). \tag{6}$$

Since the spectral peak of PXR is very narrow at $b^{(s)}\gg 1$, integration in (6) can be implemented with the use of the well-known approximation: $\dfrac{\sin^2(Tx)}{x^2}\to\pi T\delta(x)$. After integration, angular distribution (6) takes the form

$$\frac{dN_{\text{PXR}}^{(s)\text{din}}}{d\Omega}=\frac{e^2\omega_B\chi_g'^2C^{(s)^2}P^{(s)^2}}{4\pi\sin^2\theta_B} \times\frac{\varepsilon^2\theta^2}{\chi_g'^2C^{(s)^2}+\varepsilon\left(\theta^2+\gamma^{-2}-\chi_0'\right)^2}\frac{L}{\sin(\delta-\theta_B)}. \tag{7}$$

Let us consider the well-know expressions describing the PXR angular density in the kinematic approach [5, 15]:

$$\frac{dN_{\text{PXR}}^{(s)\text{kin}}}{d\Omega}=\frac{e^2\omega_B\chi_g'^2C^{(s)^2}P^{(s)^2}}{4\pi\sin^2\theta_B}\frac{\theta^2}{\left(\theta^2+\gamma^{-2}-\chi_0'\right)^2}\Gamma(\varepsilon),$$
$$\Gamma(\varepsilon)=\frac{\varepsilon}{\omega_B\chi_0''}\left(1-\exp\left(\frac{\omega_B\chi_0''L}{\varepsilon\sin(\delta-\theta_B)}\right)\right). \tag{8}$$

It is seen that asymmetry coefficient ε is contained only in the geometric factor $\Gamma(\varepsilon)$ of the kinematic expression. In the case of a thin nonabsorbing crystal, the geometric factor is an electron path in the crystalline target:

$$\Gamma(\varepsilon)=\frac{L}{\sin(\delta-\theta_B)}. \tag{9}$$

Therefore, the aforementioned kinematic expression can be written as

$$\frac{dN_{\text{PXR}}^{(s)\text{kin}}}{d\Omega}=\frac{e^2\omega_B\chi_g'^2C^{(s)^2}P^{(s)^2}}{4\pi\sin^2\theta_B} \times\frac{\theta^2}{\left(\theta^2+\gamma^{-2}-\chi_0'\right)^2}\frac{L}{\sin(\delta-\theta_B)}. \tag{10}$$

It should be emphasized that the dynamic formula differs from the kinematic one in that asymmetry parameter ε (angle δ) is contained not only in expression (9) defining an electron path in the plate, but also in the multiplicand describing the PXR angular distribution. Hence, such a difference can serve as a base to compare the dynamic and kinematic formulas derived for a thin crystal.

In subsequent analysis, it is convenient to use expressions (7) and (10) rewritten as follows:

$$\frac{dN_{\text{PXR}}^{(s)\text{din}}}{d\Omega}=\frac{e^2\omega_B\left|\chi_g'\right|C^{(s)}P^{(s)^2}}{4\pi\sin^2\theta_B}\cdot\frac{L}{\sin(\delta-\theta_B)}F^{\text{din}}, \tag{11a}$$

$$F^{\text{din}}=\nu^{(s)}\frac{\varepsilon^2\dfrac{\theta^2}{\left|\chi_0'\right|}}{\nu^{(s)^2}+\varepsilon\left(\dfrac{\theta^2}{\left|\chi_0'\right|}+\dfrac{1}{\gamma^2\left|\chi_0'\right|}+1\right)^2}, \tag{11b}$$

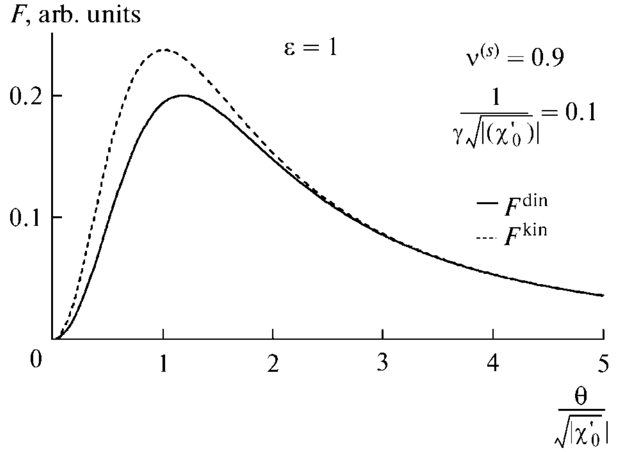

Fig. 2. Comparison between the PXR angular density curves constructed from dynamic and kinematic formulas. The kinematic formula provides an error under the given conditions.

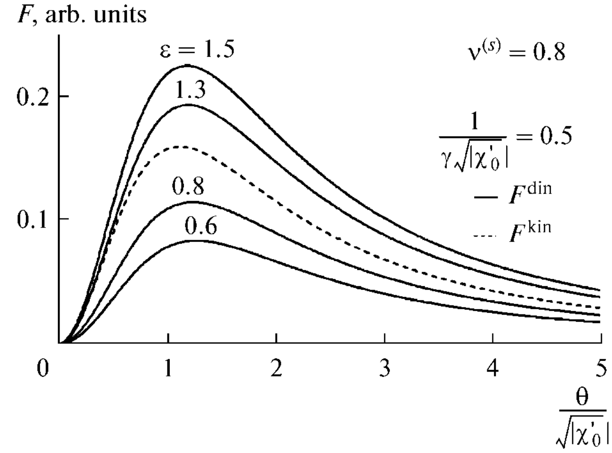

Fig. 3. PXR angular density curves calculated at different degrees of asymmetry. It is seen that the error of the kinematic formula increases with growing asymmetry.

$$\frac{dN_{\rm PXR}^{(s)\rm kin}}{d\Omega} = \frac{e^2\omega_{\rm B}|\chi'_g|C^{(s)}P^{(s)^2}}{4\pi\sin^2\theta_{\rm B}} \cdot \frac{L}{\sin(\delta-\theta_{\rm B})}F^{\rm kin}, \quad (12a)$$

$$F^{\rm kin} = \nu^{(s)}\frac{\frac{\theta^2}{|\chi'_0|}}{\left(\frac{\theta^2}{|\chi'_0|}+\frac{1}{\gamma^2|\chi'_0|}+1\right)^2}. \quad (12b)$$

Functions (11b) and (12b) define PXR angular densities and confirm the fact that only the dynamic approach allows for the influence of asymmetry on the angular component of the PXR distribution.

Symmetric Reflection

Let us consider the features of symmetric reflection at $\varepsilon = 1$. At all observation angles θ, the approximate equality $F_{\rm din} \approx F_{\rm kin}$ holds true if an emitting particle has the low energy $\gamma \le \frac{1}{\sqrt{|\chi'_0|}} \approx \frac{\omega}{\omega_p}$ (ω_p is the plasma frequency.)

In the case of weak reflections (e.g., $\nu^{(s)} \approx 0.3$), $F_{\rm din} \approx F_{\rm kin}$ if the particle energy is very high ($\gamma \gg \omega/\omega_p$). In the presence of strong reflections (e.g., $\nu^{(s)} \approx 0.9$), the angular density dependences constructed from dynamic and kinematic formulas are somewhat different (Fig. 2). In this case, kinematic formulas provide an error in the absolute yield of photons. Hence, when the absolute yield of PXR is measured with a sufficient accuracy, the results must be compared to dynamic formula (7).

Asymmetric Reflection

In the presence of reflection asymmetry caused by either a decrease ($\varepsilon > 1$) or an increase ($\varepsilon < 1$) in the angle $(\delta - \theta_{\rm B})$ of electron incidence on the target (Fig. 1), the kinematic formula error increases, as is illustrated by the curves in Fig. 3. In the case of strong asymmetry ($\varepsilon \gg 1$), i.e., at the small angle $(\delta - \theta_{\rm B})$ of electron incidence on the target, the ratio of (11b) and (12b) is

$$\frac{F_{\rm din}}{F_{\rm kin}} = \varepsilon. \quad (13)$$

irrespective of whether the Lorentz factor is greater or less than ω/ω_p. Therefore, strong asymmetry implies that the PXR angular density is ε times as large as the density predicted by the kinematic formula (Fig. 4).

Thus, even if a thin nonabsorbing crystal is investigated, it is necessary to allow for the dynamic effects of PXR.

COMPARATIVE ANALYSIS OF KINETIC AND DYNAMIC FORMULAS: A THICK ABSORBING CRYSTAL

In comparative analysis it is convenient to use expressions (1) and (8) represented as

$$\frac{dN_{\rm PXR}^{(s)\rm din}}{d\Omega} = \frac{e^2P^{(s)^2}}{4\pi\sin^2\theta_{\rm B}}F_{\rm abs}^{\rm din}, \quad (14a)$$

$$F_{\rm abs}^{\rm din} = \nu^{(s)}\frac{\frac{\theta^2}{|\chi'_0|}}{\left(\frac{\theta^2}{|\chi'_0|}+\frac{1}{\gamma^2|\chi'_0|}+1\right)^2}\frac{1}{2\pi}\int_{-\infty}^{+\infty}R_{\rm PXR}^{(s)}d\eta^{(s)}(\omega), \quad (14b)$$

$$R_{\text{PXR}}^{(s)} = \left(1 - \frac{\xi^{(s)}}{\sqrt{\xi^{(s)^2} + \varepsilon}}\right)^2 \frac{1 + \exp\left(-L_f \mu^{(s)}\right) - 2\exp\left(-\frac{L_f \mu^{(s)}}{2}\right)\cos\left(\frac{L_{e^-}}{2L_{\text{ext}}}\left(\sigma^{(s)} + \frac{\xi^{(s)} - \sqrt{\xi^{(s)^2} + \varepsilon}}{\varepsilon}\right)\right)}{\left(\sigma^{(s)} + \frac{\xi^{(s)} - \sqrt{\xi^{(s)^2} + \varepsilon}}{\varepsilon}\right)^2 + \frac{L_{\text{ext}}^2 \mu^{(s)^2}}{\varepsilon^2}}, \quad (14c)$$

$$\frac{dN_{\text{PXR}}^{(s)\text{kin}}}{d\Omega} = \frac{e^2 P^{(s)^2}}{4\pi \sin^2\theta_B} F_{\text{abs}}^{\text{kin}}, \quad (15a)$$

$$F_{\text{abs}}^{\text{kin}} = \nu^{(s)} \frac{\frac{\theta^2}{|\chi_0'|}}{\left(\frac{\theta^2}{|\chi_0'|} + \frac{1}{\gamma^2 |\chi_0'|} + 1\right)^2} \frac{\varepsilon}{\rho^{(s)}}\left(1 - \exp(-L_f \mu_0)\right), \quad (15b)$$

Here,

$$\mu^{(s)} = \mu_0 \left(\frac{\varepsilon + 1}{2} - \frac{1 - \varepsilon}{2} \frac{\xi^{(s)}}{\sqrt{\xi^{(s)^2} + \varepsilon}} - \frac{\varepsilon \kappa^{(s)}}{\sqrt{\xi^{(s)^2} + \varepsilon}}\right),$$

$$\mu_0 = \omega_B \chi_0'', \quad \sigma^{(s)} = \frac{1}{\nu^{(s)}}\left(\frac{\theta^2}{|\chi_0'|} + \frac{1}{\gamma^2 |\chi_0'|} + 1\right). \quad (16)$$

where the effective coefficient $\mu^{(s)}$ of photon absorption depends on asymmetry parameter ε of a crystal and parameter $\kappa^{(s)}$ characterizes the effect of anomalously low photoabsorption (the Bormann effect) [16] arising when X-ray waves propagate through the crystal. Its physical mechanism consists in the formation of an incident standing wave scattered by X rays, the antinodes of which are equidistant from neighboring atomic planes. At these points, the electron density of the crystal is at its minimum and, consequently, the photoabsorption has the lowest level. In addition, anomalously strong absorption of one of two waves generated in the crystal and anomalously weak absorption of the other are observed. Expression (14) describes the PXR branch exhibiting anomalously weak absorption. As in the case of free X-ray waves, is the approximate equality between the imaginary parts of the corresponding coefficients of the Fourier expansion of its dielectric susceptibility in terms of reciprocal lattice vectors $\left(\kappa^{(s)} \approx 1\right)$ is a necessary condition of manifestation of the given PXR effect in the crystal. In this case, coefficient $\mu^{(s)}$ defined by (16) reaches its minimum. It should be remembered that parameter $\kappa^{(s)}$ depends on the chosen set of parallel diffracting atomic planes in the crystal, radiation frequency, and its polarization.

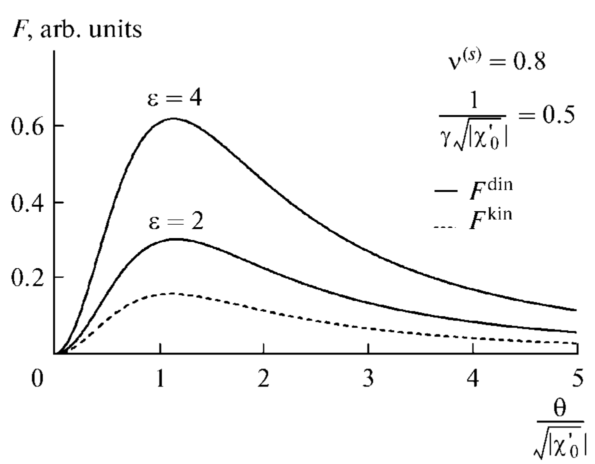

Fig. 4. PXR angular density curves calculated at different degrees of asymmetry. In the case of strong asymmetry, the PXR angular density is τ times greater than the density predicted by the kinematic formula.

Equation (4) has the solution

$$\xi^{(s)}(\omega_*) = \frac{1 - \varepsilon \sigma^{(s)^2}}{2\sigma^{(s)}}, \quad (17)$$

which determines the central frequency ω_* of the spectrum of PXR photons emitted at a fixed observation angle. Therefore, the value of effective absorption coefficient $\mu^{(s)}$ depends on observation angle θ. Since the dynamic theory allows for the influence of absorption, the PXR angular density curves constructed from the dynamic formula can be deformed with respect to the density curve calculated via the kinematic theory (Fig. 5).

The foregoing discussion enables us to draw the following inferences. In kinematic expressions (15), asymmetry affects the process geometry only and absorption coefficient μ_0 corresponds to absorption in an amorphous medium. In dynamic expressions (14), absorption coefficient $\mu^{(s)}$ depends not only on the chosen set of diffracting atomic planes of a crystal (parameter $\kappa^{(s)}$), but also on the asymmetry coefficient and the observation angle. In addition, the effective photon absorption length is $1/\mu^{(s)}$.

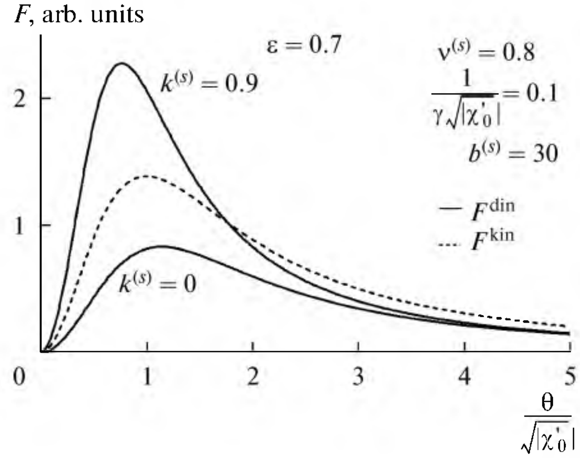

Fig. 5. Deformations of the dependence between the PXR angular density and observation angle θ observed at different values of the effective absorption coefficient.

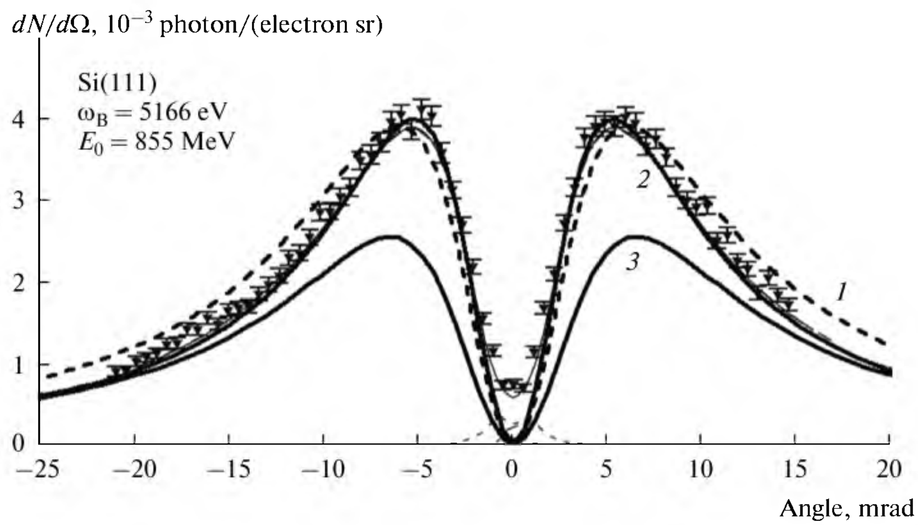

Fig. 6. Manifestation of the dynamic Bormann effect in PXR.

INTERPRETATION OF THE RESULTS OF THE EXPERIMENT ON PARAMETRIC X-RAY RADIATION OF RELATIVISTIC ELECTRONS AT THE MAINZ MICROTRON

The results of the experimental investigation into the PXR spectral-angular distribution of electrons with energies of 855 MeV have been reported in [15]. It should be noted that a high quality of the electron beam (small cross-section sizes and a low divergence) and detecting equipment of the accelerator enabled the authors of [15] to determine the angular distribution of X-ray photons in absolute units at high accuracy and angular resolution. Let us compare the results of the experiment of interest with our calculations according to well-known kinematic expressions (15) and dynamic expressions (14) derived above (Fig. 6). It is seen that dashed curve *1* corresponding to the kinematic formula differs slightly from the experimental results. Solid curve *2*, which was calculated from our dynamic formula and characterizes asymmetric photon reflection by the set of {111} planes, agrees closely with the experiment. It is important to note that the conditions of the experiment considered indicate the pronounced manifestation of the effect of anomalously low photoabsorption (the Bormann effect) in the asymmetric case of PXR [11]. This assertion is illustrated by solid curve *3* calculated from the dynamic formula without allowance for the Bormann effect.

Thus, the dynamic Bormann effect of PXR can be assumed to have occurred in this experiment.

CONCLUSIONS

Comparative analysis between the formulas of the kinematic and dynamic approaches to description of parametric X-radiation has been carried out under the conditions of symmetric and asymmetric reflections. In the case of reflection symmetry in a thin crystal (including the nonabsorbing one), the PXR kinematic formula is shown to be erroneous at the emitting particle energies $\gamma \gg \omega/\omega_p$. However, the PXR kinematic and dynamic theories provide identical results at $\gamma \gg \omega/\omega_p$. It has been found that the error of the kinematic formula increases with growing asymmetry and, moreover, the PXR angular density calculated from the kinematic formula is ε times less than the actual density predicted by the dynamic formula under the condition of strong asymmetry $(\varepsilon \gg 1)$. Thus, even if a thin nonabsorbing crystal is examined, the dynamic effects of PXR must be taken into consideration. In the case of a thick absorbing crystal, the dynamic theory enables us to calculate the PXR absorption coefficient with allowance for reflection asymmetry and the direction of photon emission, which lead to the deformation of the angular distribution shape constructed from the kinematic formula.

The developed theory has made it possible to interpret the results of the experiment on relativistic electron PXR implemented at the Mainz microtron and reveal the anomalous photoabsorption effect (the Bormann effect) in PXR.

REFERENCES

1. M. L. Ter-Mikaelyan, *The Influence of the Medium on High-Energy Electromagnetic Processes* (AN ArmSSR, Yerevan, 1969) [in Russian].
2. G. M. Garibyan and Yan Shi, Zh. Eksp. Teor. Fiz. **61**, 930 (1971) [J. Exp. Theor. Phys. **34**, 495 (1971)].
3. V. G. Baryshevskii and I. D. Feranchuk, Zh. Eksp. Teor. Fiz. **61**, 944 (1971) [J. Exp. Theor. Phys. **34**, 502 (1971)].
4. H. Nitta, Phys. Lett. A **158**, 270 (1991).
5. I. D. Feranchuk and A. V. Ivashin, J. Phys. **46**, 1981 (1985).
6. V. G. Baryshevsky and I. D. Feranchuk, J. Phys. **44**, 913 (1983).
7. A. S. Kubankin, N. N. Nasonov, V. I. Sergienko, and I. E. Vnukov, Nucl. Instrum. Methods Phys. Res. B **201**, 97 (2003).
8. N. Nasonov and A. Noskov, Nucl. Instrum. Methods. Phys. Res. B **201**, 67 (2003).
9. S. Blazhevich and A. Noskov, Nucl. Instrum. Methods. Phys. Res. B **252**, 69 (2006).
10. S. Blazhevich and A. Noskov, Nucl. Instrum. Methods. Phys. Res. B **266**, 3770 (2008).
11. S. V. Blazhevich and A. V. Noskov, Nucl. Instrum. Methods. Phys. Res. B **266**, 3777 (2008).
12. A. N. Aleinik, A. N. Baldin, E. A. Bogomazova, et al., Pis'ma Zh. Eksp. Teor. Fiz. **80**, 447 (2004) [JETP Lett. **80**, 393 (2004)].
13. S. V. Blazhevich and A. V. Noskov, Poverkhnost', No. 4, 40 (2010) [J. Surf. Invest. **4**, 303 (2010)].
14. Z. G. Pinsker, *Dynamical Scattering of X-rays in Crystals* (Nauka, Moscow, 1974; Springer-Verlag, Berlin, 1978).
15. K.-H. Brenzinger, C. Herberg, B. Limburg, et al., Physica A **358**, 107 (1997).
16. G. Borrmann, Zh. Phys **42**, 157 (1941).